ARTICLE

OBC
www.rsc.org/obc

Water soluble sapphyrins: potential fluorescent phosphate anion sensors †

Jonathan L. Sessler,*[a] Julian M. Davis,[a] Vladimir Král,[b] Thomas Kimbrough[a] and Vincent Lynch[a]

[a] *Department of Chemistry and Biochemistry and Institute for Cellular and Molecular Biology, 1 University Station, The University of Texas at Austin, Austin, Texas 78712, USA*

[b] *Department of Analytical Chemistry, Institute of Chemical Technology, Technická 5, 166 28 Prague, Czech Republic*

Received (in Pittsburgh, PA, USA) 23rd June 2003, Accepted 12th September 2003
First published as an Advance Article on the web 13th October 2003

As part of an ongoing effort to study the anion binding properties of sapphyrins in various media, a number of previously reported water solubilized sapphyrins were studied in methanol and in buffered, neutral aqueous solutions and found to undergo self-aggregation under these solution phase conditions. The nature of the species produced as the result of self-aggregation and the processes leading to their formation were studied *via* UV-vis absorbance and fluorescence spectroscopy. In previous work (V. Král, H. Furuta, K. Shreder, V. Lynch, and J. L. Sessler, *J. Am. Chem. Soc.*, 1996, **118**, 1595–1607.) it was found that the addition of phosphate-type anions to water soluble sapphyrins at pH 6.1 gives rise to visible spectroscopic changes consistent with the binding to the aggregated form and the concurrent formation of an anion-bound dimer with effective equilibrium constants on the order of 100–300 M^{-1}. In this study we show that at high phosphate-to-sapphyrin ratios in neutral, buffered aqueous solutions further deaggregation occurs to produce an anion-bound monomeric form. This highly fluorescent species is formed with effective equilibrium constants on the order of 6–19 M^{-1} leading to considerations that sapphyrins could function as fluorescent phosphate anion sensors. In an effort to modulate the deaggregation properties, several new sapphyrin derivatives bearing two meso aryl substituents were prepared and studied. The aggregation properties of these latter systems were analyzed in methanol and, in the case of one water solublized system, in neutral aqueous media. In analogy to what was observed for the β-alkyl substituted sapphyrins, H-type aggregates were seen for the water solubilized meso-substituted system in aqueous media. However, in contrast to the H-type dimers seen in the case of the meso-free systems in methanol, J-type dimers were observed in the case of the sapphyrins bearing two meso substituents in this solvent. The effective dimerization constants of several of the meso-diaryl sapphyrins were determined in methanol as were their pK_a values in aqueous media. The solid state structure of the bis HBr salt of one of the meso-diaryl sapphyrins, specifically 10,15-bis(3,5-di-*tert*-butylphenyl)-3,22-diethyl-2,23-dimethylsapphyrin, was also determined and found to show elements in common with those of previously reported sapphyrin derivatives. In particular, the two counter anions were found to be hydrogen bound above and below the diprotonated sapphyrin plane.

Introduction

The porphyrins are among the widely studied and most versatile of all macrocyclic compounds and are currently seeing application in areas as diverse as medicine, materials science, and analyte sensing.[1–3] In fact, the functional utility and practical importance of the porphyrins continue to inspire research across a wide range of disciplines and have led, among other things, to the synthesis of many new porphyrin analogues, including so-called "expanded porphyrins". Expanded porphyrins are synthetic polypyrrolic macrocycles that bear analogy to the porphyrins but are larger in size.[4,5] As a class, they exhibit a variety of interesting properties, including an ability to bind, sense, transport, and separate anions.[4,5]

Understanding the anion binding behavior of expanded porphyrins requires an appreciation of their chemical nature in the absence of anions, in particular whether they exist in monomeric or aggregated forms. Porphyrins are well known to undergo dimerization and aggregation under a variety of conditions and have been the subject of considerable study inspired in part by a desire to understand the nature of the nonmonomeric chromophores involved in photosynthesis and other light-harvesting processes.[6–11] By contrast, relatively little effort has been devoted to studying the dimerization and aggregation properties of expanded porphyrins. Thus far, the only expanded porphyrin whose aggregation properties has been examined is sapphyrin (*e.g.*, **1**), and only under a limited set of conditions.[12–14] The sapphyrins are the oldest and perhaps best known of the expanded porphyrins.[4,5,15,16] They are pentapyrrolic macrocycles that contain a 22 π-electron aromatic periphery that have been shown to bind several classes of anions under a range of solution phase conditions, as well as in the solid state. Here, the recognition of phosphate anions and their derivatives (*e.g.*, nucleotides) has received particular attention, having been studied by a variety of methods, including transport experiments and titrations monitored by UV-vis, ^{1}H- and ^{31}P-NMR.[13,14,17–19] In aqueous media, the binding of organic phosphate-type anions (*e.g.*, phenylphosphonate, mononucleotides) by water-solubilized, β-pyrrole-substituted sapphyrins has been linked to changes in the aggregation state of the sapphyrins.[14] In previous work, it was found, for instance, that the addition of phenylphosphonate to water-soluble sapphyrin **1** at pH 6.1 gave rise to visible spectroscopic changes consistent with the breakup of an initial aggregated form and the concurrent formation of an anion-bound dimeric species. The effective equilibrium constant for this process was found to be 310 M^{-1}.[13] Not addressed in this study was what happened at high anion-to-sapphyrin ratios. However, associated qualitative

† Electronic supplementary information (ESI) available: dependence of fluorescence variables on sapphyrin concentration. See http://www.rsc.org/suppdata/ob/b3/b306964h/

DOI: 10.1039/b306964h

studies led to the consideration that the anion-bound monomeric form could be obtained by adding a surfactant or in the presence of a protic organic solvent such as methanol.[13,14] The monomeric form was also observed in the presence of DNA at high phosphate-to-sapphyrin ratios.[14] Subsequent to these initial studies, we discovered that the monomeric form of sapphyrin is appreciably fluorescent whereas the aggregated and dimeric forms are not. This led to the consideration that de-aggregation events at high phosphate-to-sapphyrin ratios could be followed by fluorescence emission spectroscopy. To the extent that an appreciable change in fluorescence could be correlated to corresponding changes in phosphate concentration, the sapphyrins could find utility as possible water-soluble fluorescent phosphate anion sensors. Recently, we have found that water-solubilized sapphyrins localize effectively to neoplastic tissues,[20] underscoring the potential benefits of having such sapphyrin-based sensors. In this paper we show that adding large quantities of inorganic phosphate to pH 7.0 solutions of various water-solubilized sapphyrins gives rise to fluorescence emission consistent with the formation of an anion-bound monomeric form. Effective equilibrium constants for this process were found to range from 5.6 to 19 M^{-1}. Also reported here is the synthesis of two new meso-diaryl sapphyrins, the X-ray structural characterization of the bis-HBr salt of one of these products, as well as their dimerization behavior in methanol.

Results and discussion

Synthesis

Several water-soluble sapphyrin derivatives (**1**–**9**) were chosen for use in this study. These specific systems were selected because they were all freely soluble (although not necessarily monomeric) at the concentrations required for optical studies ([sapphyrin] < 10^{-5} M) and because it was thought that when studied as a group they would allow the effects of various water-solubilizing groups, overall macrocycle charge, and steric bulk on the aggregation and anion binding behavior of sapphyrins to be examined in detail.

Sapphyrin **1** and the polyamine sapphyrins **2**–**4** were prepared according to literature procedures.[13,20,21] The decahydroxy sapphyrins **5** and **6** were prepared *via* the EDC mediated coupling of sapphyrin diacid **10** with D-glucamine (**11**) and N-methyl-D-glucamine (**12**), respectively, as shown in Scheme 1. The yields of these reactions, 13% for **5** and 10% for **6**, were low primarily due to loss of product during purification.

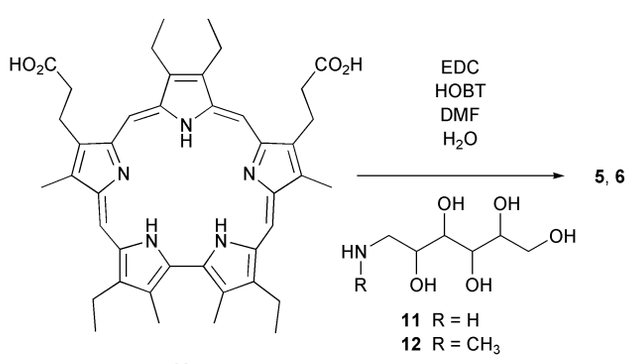

Scheme 1

The two synthetic routes previously reported for the synthesis of 10,15-diaryl sapphyrins (*e.g.*, **7**), summarized in Scheme 2,[22,23] were used to synthesize the new meso-substituted sapphyrin **9**. Method A involves a [3 + 2] acid catalyzed condensation of a diaryl tripyrrane (*e.g.*, **13** or **14**) with a bisformyl bipyrrole (*e.g.*, **15**) followed by oxidation.[22] In Method B, the tripyrrane subunit of sapphyrin is formed *in situ*, by combining

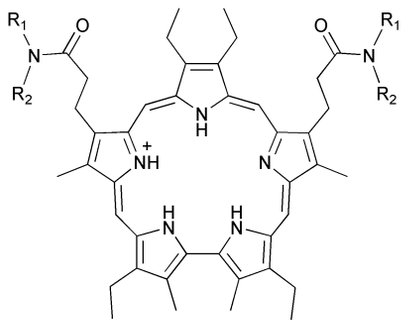

1 $R_1 = R_2 = A$
2 $R_1 = H$, $R_2 = B$
3 $R_1 = H$, $R_2 = C$
4 $R_1 = H$, $R_2 = D$
5 $R_1 = H$, $R_2 = E$
6 $R_1 = CH_3$, $R_2 = F$

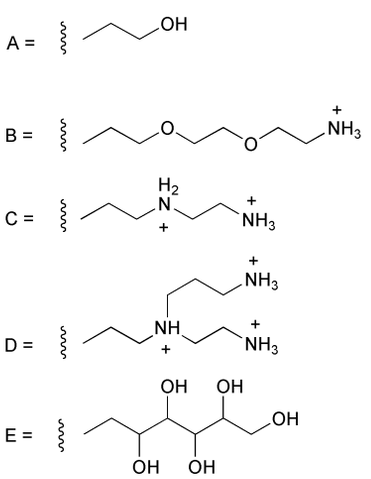

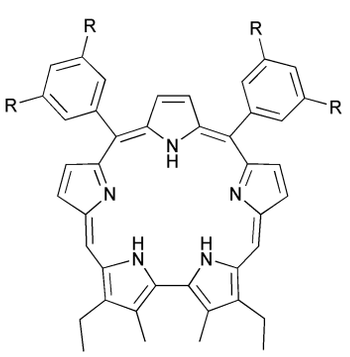

7 R = H
8 R = *t*-Bu
9 R = PEG

pyrrole, an aromatic aldehyde, and bisformyl bipyrrole in a 3:2:1 ratio under acid catalyzed conditions followed by oxidation to give the 10,15-diaryl sapphyrins **7**–**9**.[23] The preparation of the diaryl system **7** has been previously reported both by the 'one-pot' method[23] and the [3 + 2] method,[22] with the first of these procedures proving superior for the present purposes. In fact, the yield of sapphyrin **9** (9%) obtained using the [3 + 2] (Method A) proved only slightly higher in our hands than the 6% yield obtained using the 'one pot' (Method B). Further, due to the presence of porphyrin and other polypyrrolic side products, the requirement for extensive chromatographic workup associated with this ostensibly 'cleaner' [3 + 2] procedure proved no different from that for the 'one pot' approach (Method B). These two observations, namely the low yield and the formation of relatively impure crude product, lead us to suggest that the bonds between the α-pyrrolic carbons and

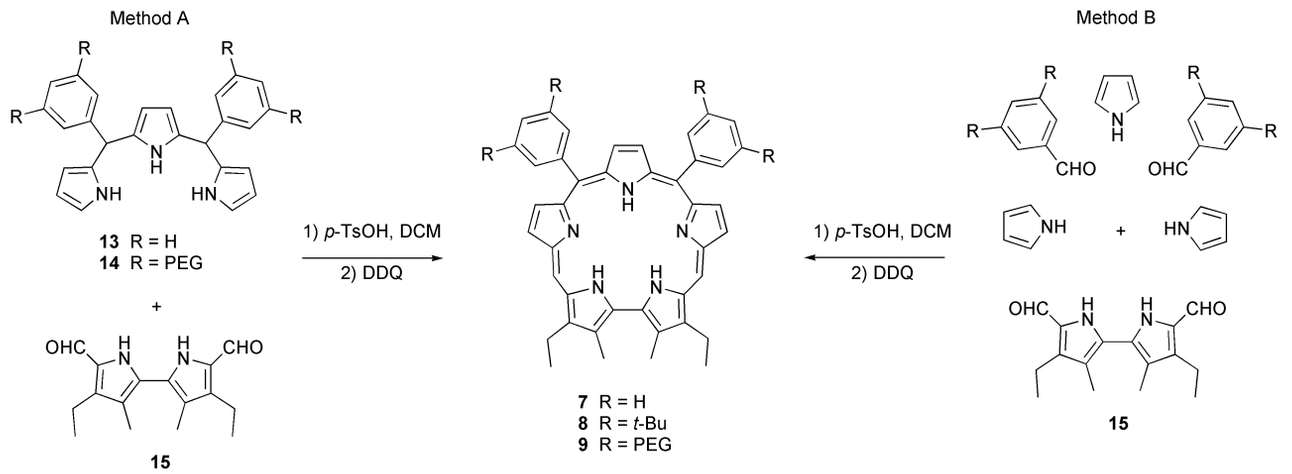

Scheme 2

meso-carbons of tripyrrane **14** are labile under the acid-catalyzed conditions of the reaction and that this key intermediate might in fact be falling apart prior to reacting with the dialdehyde **15**.

Since the preparation of diaryl tripyrranes, such as **14**, requires extensive purification by column chromatography but does not impart any benefit as far as final product clean-up is concerned, the 'one-pot' approach (Method B) was chosen as the preferred one for the synthesis of sapphyrins **8** and **9**. In the case of both targets, the reactants were combined in dichloromethane and treated with a catalytic amount of *p*-toluenesulfonic acid (*p*-TsOH). The reaction mixtures were stirred in the absence of light overnight at room temperature, followed by the addition of 2,3-dichloro-5,6-dicyanobenzoquinone (DDQ). After workup, the crude products were purified by column chromatography, first over alumina and then twice over silica gel, using a mixture of methanol (0.2–8%) in dichloromethane as the eluent for both solid phases. The yields (5% for **8**, 6% for **9**) were similar to those reported for other diaryl sapphyrins prepared *via* this 'one pot' procedure (*e.g.*, 8% for **7**).[23] Not surprisingly, significant amounts of porphyrin were isolated from the reactions used to produce the 10,15-diaryl sapphyrins. One of the products, compound **16**, represents a porphyrin system that has not apparently been reported previously. It was thus fully characterized as detailed in the experimental section.

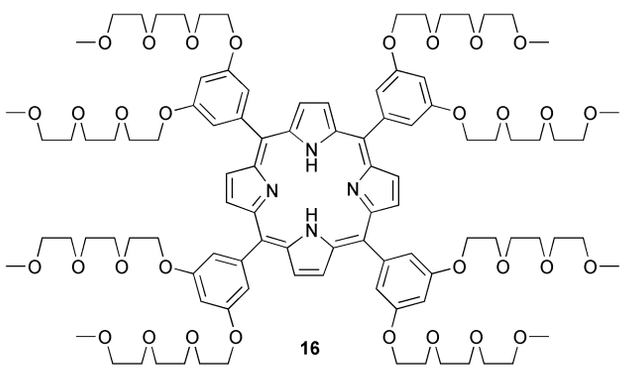

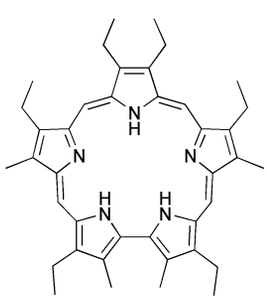

Aggregation/anion binding studies

In previous work, we characterized three distinct aggregation states for sapphyrins in polar, protic media.[13,14] These states can be clearly distinguished by their UV-vis absorbance features. This is evident by inspection of Fig. 1, which depicts the spectra of sapphyrin **6** in 10 mM PIPES buffer (pH 7.0) in the presence of 0, 0.1, and 10 mM sodium dodecyl sulfate (SDS), a well-known surfactant. The monomer has a strong, sharp Soret-like absorbance around 450 nm. The Soret-like band of the dimer appears around 420 nm in the absorbance spectrum and is broadened relative to that of the monomer. It is also less intense. The higher order aggregates, referred to herein simply as "aggregates", have a collective absorbance centered around 410 nm. The absorbance maxima of these aggregates shift to the red upon dilution, a feature that is characteristic of H-type (face-to-face) aggregation.[24] The monomer is highly fluorescent, much more so than either the dimer or aggregate form. Examination of the excitation spectra of these three solutions reveals an emission intensity maxima from each solution at the excitation wavelength corresponding to the absorbance maximum of the monomeric form, indicating that a significant portion of the emission from the solutions containing dimers and higher-order aggregates actually comes from the small amounts of monomer present in these solutions.

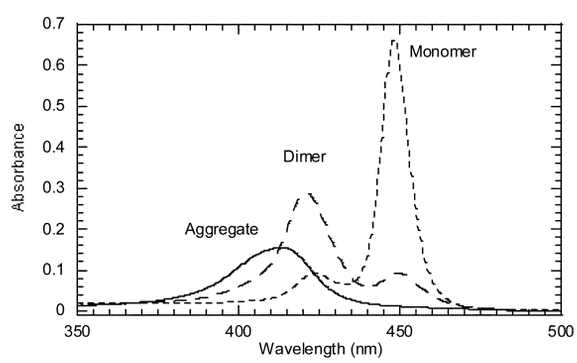

Fig. 1 Absorbance spectra of sapphyrin **6** (3 μM) as recorded in 10 mM PIPES buffer (pH 7.0) in the presence of 0, 0.1, and 10 mM sodium dodecyl sulfate (SDS). These spectra are ascribed to the presence of three different prominent aggregations states, monomer, dimer, and "aggregate"; see text for details.

The dominant forms of phosphate anions in neutral aqueous media are $H_2PO_4^-$ and HPO_4^{2-}, which exist in an approximately 3:2 ratio at pH 7.0 (for H_3PO_4: $pK_{a1} = 2.1$, $pK_{a2} = 7.2$, $pK_{a3} = 12.3$).[25] These two forms are referred to collectively herein

simply as "phosphate," "sodium phosphate," or as P_i, when referring to their corresponding sodium salts. Based on results of previous studies, it was expected that the addition of sodium phosphate to aqueous pH 7.0 solutions of sapphyrin would shift the aggregation equilibrium towards first the dimeric and subsequently the monomeric forms, respectively, presumably because of binding interactions between the cationic sapphyrin macrocycle and the phosphate anions. In accord with the earlier, quantitative analysis of phosphate-type anions interacting with **1** at pH 6.1, it was found that addition of inorganic phosphate to this sapphyrin at pH 7.0 in the absence of external buffer gave rise to large changes in the visible absorption spectrum at relatively low phosphate-to-sapphyrin ratios. Over this concentration regime, relatively little change was observed in the fluorescence emission spectrum. However, as the phosphate-to-sapphyrin ratios were raised, a substantial increase in the emission intensity at 690 nm was observed, indicative of formation of a monomeric sapphyrin species. These spectral changes, reproduced in Fig. 2, support the contention that several regimes, in which different equilibrium processes dominate, may be defined over the course of the overall sapphyrin aggregate + phosphate --> sapphyrin–phosphate monomer deaggregation process, with the last of these most readily visualized by fluorescence spectroscopy corresponding to the phosphate-induced production of the monomer.

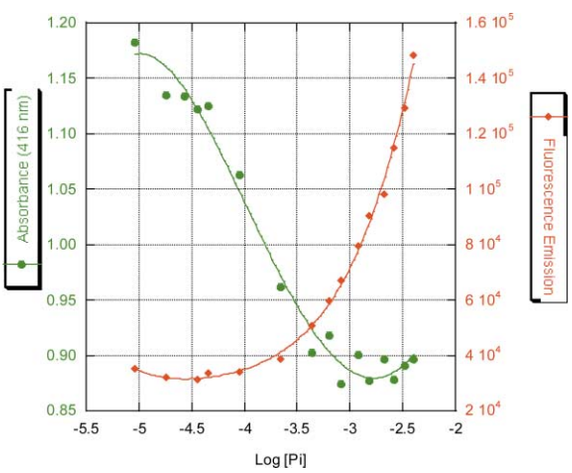

Fig. 2 Change in absorption (at 416 nm) and emission (λ_{ex} = 450 nm, λ_{obs} = 692 nm) intensity observed when 6.6 μM aqueous pH 7.0 solutions of sapphyrin **1** containing no external buffer or other additives are titrated with increasing concentrations of sodium phosphate (P_i). The curves through the experimental data points are arbitrary and meant to aid in visualization.

The observation of a phosphate-induced increase in fluorescence intensity leads to the consideration that water-soluble sapphyrins such as **1** could be used as phosphate-anion sensors. However, the ultimate application of such systems in biological milieus requires at test of the aggregation–deaggregation behavior under more physiological conditions. As a first effort to model such conditions, in this study we have elected to analyze the phosphate-induced deaggregation and monomerization of several water-soluble sapphyrins at pH 7.0 in the presence of 150 mM NaCl using 25 mM PIPES buffer to maintain neutral pH.‡ Under these conditions, as will be detailed below, the demarcation between changes in the visible spectrum at low phosphate-to-sapphyrin ratios and the fluorescence emission increase observed at higher ratios became less distinct. Nonetheless, as was true in the absence of buffer and chloride, it was changes in the emission, rather than absorption, spectra that dominated at high phosphate-to-sapphyrin ratios.

Fig. 3 shows the effect of the addition of aliquots of phosphate, up to 50 mM at pH 7.0, on the Soret-like band of a 6.6 μM solution of sapphyrin **1** in 25 mM PIPES buffer (pH 7.0) containing 150 mM NaCl. Under these conditions, where the pH and overall sapphyrin concentration are held constant, the only discernible absorbance maxima (at 415 nm) is that attributed to the higher order aggregates. This spectral feature is found to decrease in intensity and shift to the red slightly as the phosphate anion concentration is increased up to 50 mM. At higher concentrations of phosphate (>100 mM), an absorbance maximum around 425 nm, attributed to the dimeric form, is seen to grow in. On the other hand, an increase in the fluorescence emission intensity of the sapphyrin solution was found over the full course of the titration ($0 < [P_i] < 180$ mM), with these changes being somewhat more appreciable at the higher phosphate-to-sapphyrin ratios, as can be seen from an inspection of Fig. 4. Similar spectral changes were seen for the other water-soluble sapphyrins of this study. Depending on the structure, the amount of phosphate needed to produce an appreciable increase in the fluorescence emission intensity was found to vary slightly. Likewise, the specific absorption spectral

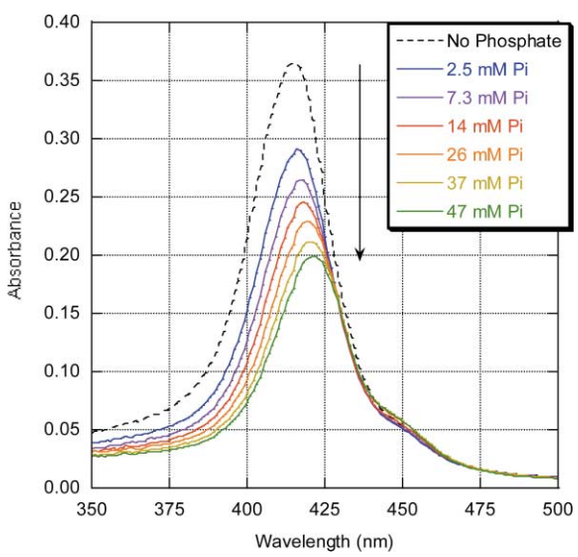

Fig. 3 Absorbance spectra of aqueous solutions of sapphyrin **1** (2.7 μM) containing 0–50 mM sodium phosphate at pH 7.0, 25 mM PIPES buffer, and 150 mM NaCl.

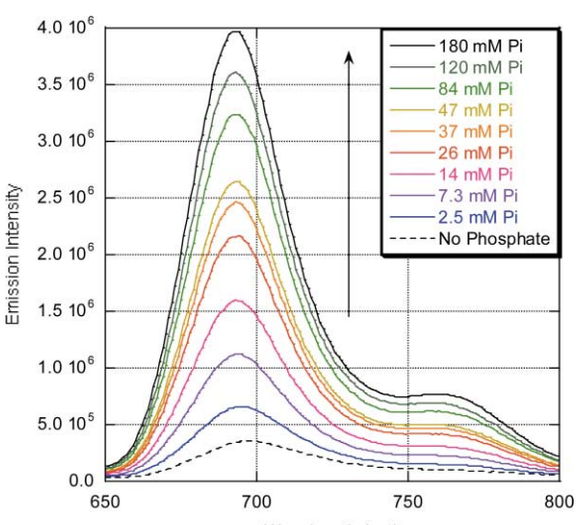

Fig. 4 Fluorescence emission spectra (λ_{ex} = 450 nm) of aqueous solutions of sapphyrin **1** (2.7 μM) containing 0–180 mM sodium phosphate at pH 7.0, 25 mM PIPES buffer, and 150 mM NaCl.

‡ In carrying out these titrations, it was considered desirable to control the pH using a buffer since the visible absorbance and fluorescence emission spectra of sapphyrins have proved to be very sensitive to small changes in pH.[14]

Table 1 Effective equilibrium constants for the phosphate anion-induced monomerization of sapphyrins **1**–**6** in buffered aqueous solutions (25 mM PIPES, 150 mM NaCl, pH 7.0)

Sapphyrin	Sapphyrin charge	Effective equilibrium constant/M^{-1}
1	+1	19 ± 3
2	+3	5.6 ± 0.3
3	+5	7.4 ± 1.0
4	+7	6.5 ± 0.5
5	+1	19 ± 2
6	+1	14 ± 2

features varied slightly from sapphyrin to sapphyrin. For instance, in the case of sapphyrin **6** (3 μM, 25 mM PIPES buffer, 150 mM NaCl, pH 7.0), the buildup of an absorption band corresponding to the dimer was observed to start at a phosphate concentration of *ca*. 10 mM.

As expected, excitation spectral studies (data not shown) reveal that the emission intensity for the water-soluble sapphyrins **1**–**6** is maximal at an excitation wavelength corresponding to the absorbance maximum of the corresponding monomeric sapphyrin (*ca*. 450 nm). Such an observation provides important support for the contention that the observed emission comes primarily from the monomeric form, rather than from the dimer or aggregate. We thus conclude that the increase in emission induced by the addition of phosphate is caused by the release of small amounts of the highly fluorescent monomeric form from the aggregates. Since this change is related to phosphate binding, and is a function of phosphate concentration, an apparent equilibrium constant for the interaction between sapphyrin and phosphate can be determined by relating the change in fluorescence emission to the phosphate anion concentration. This was done by standard curve fitting procedures assuming a 1 : 1 binding model, as described in the experimental section. The resulting values for this and the other water-soluble sapphyrins of this study are given in Table 1.

When considered in concert, the affinity constants tabulated in Table 1 lead to the conclusion that phosphate is bound more tightly by sapphyrins **1**, **5** and **6** than by the polyamine substituted systems **2**–**4**, at least as far as production of the monomer is concerned. Such a finding is consistent with the rather distant protonated amine moieties contributing little to the overall anion binding process. It is also consistent with the aggregation equilibrium of the more highly charged polyamines **2**–**4** being less affected by the presence of phosphate.

Sapphyrins are known to bind chloride anion *ca*. 40 times more weakly than phosphate in methanol.[13,27] Typical cellular concentrations of chloride are around 150 mM, as compared to 0.1–10 mM for phosphate,[28] and it was for this reason that solutions containing 150 mM NaCl were used in the present phosphate-based deaggregation studies as noted above. However, realistic as these conditions were meant to be, we were also keen to probe the effect of chloride anion on the binding process *per se*. Toward this end, aqueous, buffered solutions of sapphyrin (pH 7.0) were made up and studied in the absence of phosphate. As a general rule, it was found that addition of sodium chloride to these solutions caused the aggregation equilibrium to shift towards the dimeric form, as illustrated in Fig. 5 for the specific case of **1**. In the case of the more solubilized systems (*e.g.*, **6**), high concentrations of chloride sufficed to shift the equilibrium completely to the dimeric form, as illustrated in Fig. 6. Noteworthy, however, was the finding that, in contrast to what proved true upon the addition of phosphate, no hint of an absorbance band associated with the monomer was observed even at high chloride anion concentrations (1 M) for any of the systems investigated. Furthermore, the emission intensity of these solutions remained relatively constant over the full range of chloride concentrations tested (*i.e.*, 0 ⟶ 1 M). We thus conclude that the 'physiological concentration' of chloride anion present in the samples chosen for quantitative

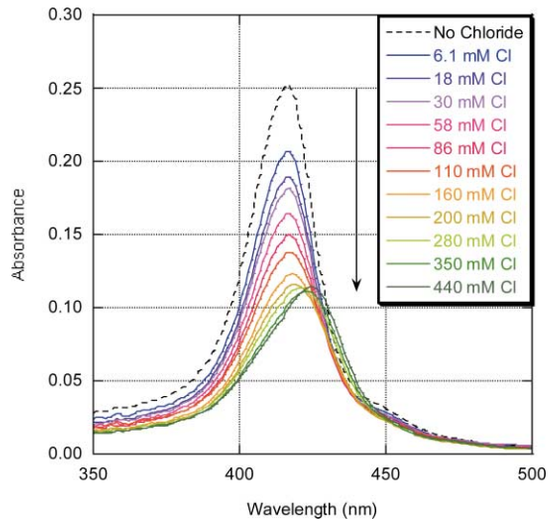

Fig. 5 Absorbance spectral changes when aqueous solutions of sapphyrin **1** (2.7 μM) at pH 7.0 are titrated with increasing concentrations (0–440 mM) of sodium chloride in 25 mM PIPES buffer.

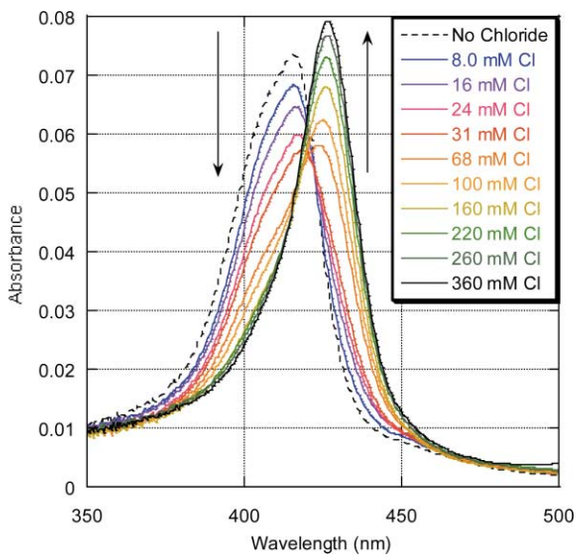

Fig. 6 Absorbance spectral changes when aqueous solutions of sapphyrin **6** (1.2 μM) at pH 7.0 are titrated with increasing concentrations (0–360 mM) of sodium chloride in 25 mM PIPES buffer.

study does not serve to interfere with the spectroscopic 'handle' used to monitor the phosphate binding process, namely augmented monomer fluorescence. Consistent with this conclusion is the finding that the effective equilibrium constant for the phosphate-induced monomerization of both sapphyrins **1** and **6** at pH 7.0 were found to be the same in 25 mM PIPES buffer with and without 150 mM NaCl.

The possible effect of sodium bromide was also studied. However, in contrast to chloride anion, the addition of NaBr to buffered solutions of sapphyrins **1**–**6** had no discernible effect on the spectroscopic profiles of these solutions. Such an observation is consistent with the expected weak bromide anion binding affinity[27] and, further, serves to rule out the possibility that the spectroscopic changes observed in the presence of phosphate and chloride anion are due simply to changes in ionic strength.

Dimerization studies

Our motivation for preparing diaryl sapphyrins **7**–**9** stemmed from a desire to understand the effect, if any, that meso-substitution could have on the stability of the various dimers and aggregates that might be formed in polar, protic media. The nature of the absorbance features observed for sapphyrin

Table 2 Dimerization constants determined for various acid salts of 10,15-diaryl sapphyrins

Sapphyrin	Dimerization constant/M^{-1}
7·2TFA	23 000 ± 4,000
7·2HCl	40 000 ± 8,000
8·2HCl	46 500 ± 8,200
9·2HCl	10 300 ± 2,100

molecules in the visible region of their spectra is known to be significantly influenced by the effects of π-stacking.[12–14] Thus, absorbance spectroscopy was used to study the dimerization behavior of diaryl sapphyrins **7**–**9** in methanol and the water soluble system **9** in neutral aqueous media. The absorbance spectra of solutions of **8**·2HCl at various concentrations in methanol, reproduced in Fig. 7, are representative of what is seen for this series of compounds and, in fact, illustrate in graphic terms the effect of π-stacking for solubilized 10,15-diaryl sapphyrins. At relatively low concentration (*e.g.*, [sapphyrin] < 1×10^{-5} M), a single absorbance maximum (at 450 nm), attributed to the monomeric form, is observed in the Soret region of the spectrum. As the concentration is increased, the apparent molar absorptivity of this absorbance band decreases, and an additional Soret absorbance (*ca.* 480 nm) emerges. This new, lower energy absorbance is attributed to a J-type dimer. In this type of dimer, the transition dipole moments of the two interacting sapphyrins are antiparallel, or head to tail, in contrast to the H-type dimers seen for the meso-unsubstituted sapphyrins **1**–**6** in this solvent, wherein the transition dipole moments of the two interacting sapphyrins are parallel to one another.[24] The novel tetra-aryl porphyrin **16** showed no propensity to form aggregates in methanol.

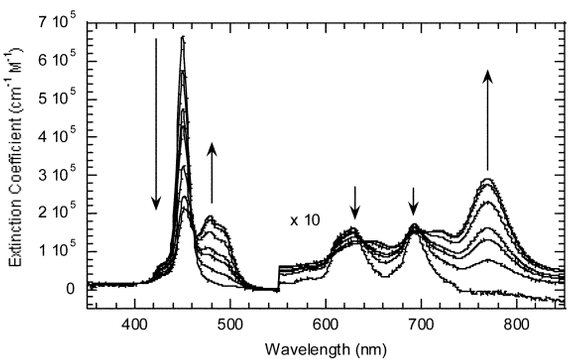

Fig. 7 Plot of apparent extinction coefficient *vs.* wavelength, for **8**·2HCl in methanol recorded in a 1 mm cuvet over a concentration range of 1.3×10^{-6} to 6.7×10^{-5} M. Changes in the Soret and Q-type bands with increasing concentration are indicated with arrows. The Q-band region (550–850 nm) is shown enlarged by a factor of 10 for clarity.

Dimerization constants for compounds **7**–**9** in methanol were determined using the method of Pasternack[29] and are summarized in Table 2. Interestingly, very similar dimerization constants were determined for both **7**·2HCl and **8**·2HCl. These two compounds differ structurally only in that the 3- and 5-positions of the meso-phenyl rings of **8** bear *t*-butyl groups whereas those of **7** do not. Thus, that similar dimerization constants were observed is perhaps not surprising, and we interpret this result to indicate that the 3,5-positions of the phenyl rings are too far removed from the overlapping porphyrin cores for steric bulk introduced at these positions to affect significantly the extent of π-stacking. However, compared to **7** and **8**, a much lower dimerization constant was determined for **9**·2HCl, a system that bears polyethylene glycol groups at the 3- and 5-positions of the meso-phenyl rings. This leads us to conclude that adding solubilizing groups at these positions inhibits π-stacking, whereas simply adding steric bulk does not.

Two additional factors were also found to affect the extent of aggregation. First, the extent of dimerization was found to be a very sensitive function of pH, with the actual spectra recorded being dependent on sample purity (*e.g.*, the presence of acid that was often retained in the samples even after extensive drying) and, of course, the actual pH. Supporting this conclusion was the finding that adding small quantities of HCl to methanolic solutions of **8** and **9** served to effect complete conversion of all but the most concentrated samples into to the corresponding monomeric forms. It was originally assumed that in methanol the monomer exists in the dicationic protonation state, and the dimer formed is between two monomeric, fully protonated dications.[12] The fact that the formation of these dimers is inhibited in the presence of acid might suggest that the dimer contains at least one sapphyrin that is not completely protonated, although evidence to support or refute this possibility has not yet been obtained. On the other hand the presence of small amounts of water (*e.g.*, 5% or less, v/v) was not found to affect the dimerization equilibrium of **8** or **9** significantly. Such a finding makes it unlikely that increases in polarity or ionic strength are responsible for the spectral changes seen in Fig. 7 (or for the large error values, *ca.* 20%, associated with the entries in Table 2).

The second factor of note is that the dimerization process is effected by anion binding, or at least the presence of certain anions. For instance, the addition of tetrabutylammonium chloride to solutions of **8**·2HCl in methanol was found to shift the dimerization equilibrium towards the monomeric form, presumably because the presence of a bound chloride ion on each face of the macrocycle inhibits π-stacking. On a more quantitative level, the dimerization constant determined for **7**·2TFA was found to be approximately half that determined for **7**·2HCl (*cf.* Table 2). Such a finding supports the notion that the nature of the anion, as well as its absolute presence, affects the extent of dimerization, even when extra equivalents of the anion are not present. Unfortunately, attempts to measure the dimerization constants of the phosphate salts of these systems were not successful because the data obtained from the requisite dilution studies did not prove sufficiently reproducible.

In contrast to what was observed in methanol, examination of the spectroscopic features of sapphyrin **9** in aqueous media revealed behavior that was best interpreted in terms of the formation of H-type dimers (or higher order aggregates) at or near neutral pH, in direct analogy to what was seen for the water soluble β-alkyl sapphyrins **2**–**6**. The fact that H-type dimers are seen in water for **9** would seem to rule out the possibility that meso-aryl substituents preclude the formation of H-type dimers. It is possible that the steric bulk from these substituents is enough to force the sapphyrin molecules to engage in a π–π interaction that leads to a red shift in the Soret band in the absorbance spectrum (J-type aggregation) under conditions, such as in methanol, where a counter anion is bound to the sapphyrin. By contrast, in aqueous solutions, where the cationic sapphyrin and its counter anion are more highly solvated, such anion-protonated interactions are less favorable and H-type aggregation dominates.

X-Ray structural analysis of a meso-diaryl sapphyrin

By recrystallizing from dichloromethane/hexane, it proved possible to obtain X-ray diffraction quality crystals of **8**·2HBr. The structure was solved in an effort to ascertain whether or not additional steric bulk at the meso-positions would affect the solid-state structure of halide anion complexes of this type (Fig. 8). Details of the core geometry for **8**·2HBr as well as, for comparison, those of **17**·2HCl and **7**·2HCl, are given in Table 3. The core NHs of sapphyrin **8** are all within hydrogen bonding distance of one of the bromide anions, with H–Br distances of 2.561 and 2.576 Å for Br1 and 2.590, 2.629, and

Table 3 X-ray structural information for **17**·2HCl, **7**·2HCl, and **8**·2HBr

Atom distances	**17**·2HCl[27]	**7**·2HCl[23]	**8**·2HBr
NH-anion (Å)[a]	2.284	2.347	2.561
	2.385	2.368	2.576
	2.438	2.401	2.590
	2.529	2.423	2.629
	2.538	2.529	2.695
Average	2.434	2.414	2.610
Anion–anion/Å	3.678(2)	3.666(2)	4.008(1)
Anion to mean sapphyrin plane/Å	1.831(3)	1.833(3)	2.003(2)
Torsion angle (°) C2–C1–C24–C23	27.7(4)	25.0(3)	27.5(9)

[a] The hydrogen atoms on the pyrrole nitrogens were calculated in idealized positions. As a result there are no esd's associated with these parameters.

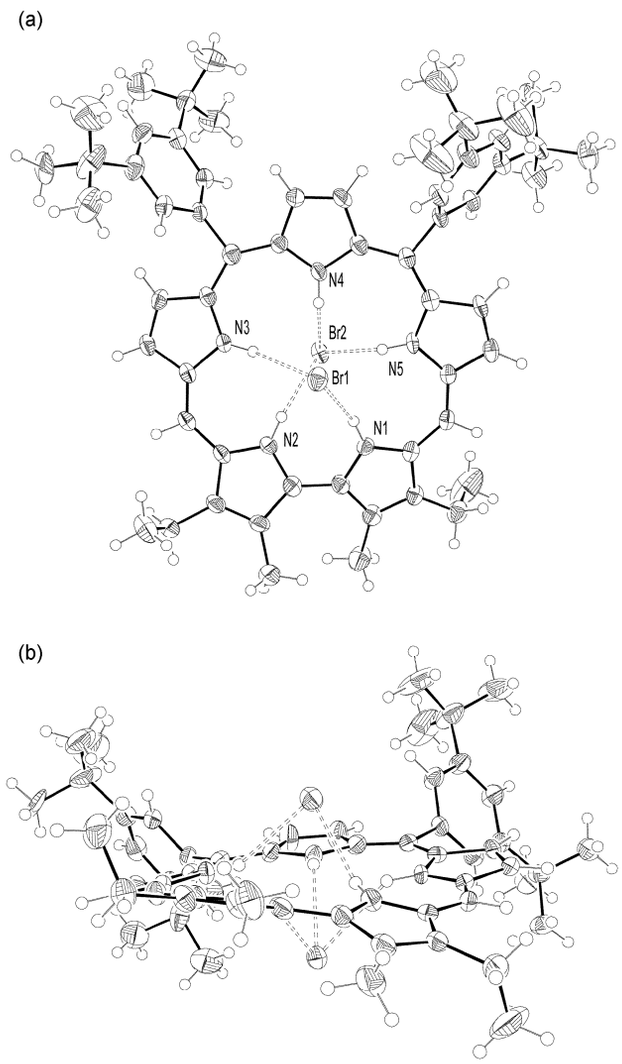

Fig. 8 Top and side views of the single crystal X-ray structure of **8**·2HBr (with probability ellipsoids shown at the 50% level).

2.695 Å for Br2. These values are slightly larger than those seen in the X-ray structures of **17**·2HCl and **7**·2HCl, a difference that can be attributed in large measure to the greater ionic radius of bromide anion relative to chloride anion (1.96 Å *vs.* 1.81 Å).[30] The bromide anions both reside 2.003 Å from the mean plane defined by the five nitrogen atoms, a distance that is slightly larger than those seen in the two sapphyrin dihydrochloride complexes characterized by X-ray diffraction analysis. The bromine anion centers are separated from each other by 4.008 Å, a distance that is slightly larger than the Cl–Cl separations found in the other structures. Again, both of these discrepancies can be accounted for by the larger ionic radius of the bromide anion relative to that of the chloride anion. It is interesting to note that in all three structures, the two anions are separated from one another by little more than twice their ionic radii. The most noticeable deviation from planarity in the macrocycle itself is the characteristic twist in the bipyrrole subunit, with a torsion angle of *ca.* 27.5°. This twist, attributed to steric interactions between the substituents at the β-positions, is similar to those seen in the X-ray structures of **17**·2HCl and **7**·2HCl.[23,27]

Protonation characteristics of meso-diaryl sapphyrin

The acid–base properties of the diaryl sapphyrin **9** were also examined. The three protonation states normally observed for sapphyrins, the free base (*e.g.*, **9**), the monoprotonated monocation (*e.g.*, $H\mathbf{9}^{+}$), and the diprotonated dication (*e.g.*, $H_2\mathbf{9}^{2+}$), are all spectroscopically distinct. The absorbance spectra of these three different protonation states of the water soluble **9** in buffered aqueous solutions are shown in Fig. 9. The absorbance and emission maxima are summarized in Table 4. As is the case for the meso-free, β-alkyl substituted sapphyrins (such as **2**–**6**), the monocationic form of **9** was found to have the highest relative emission intensity. The pK_a's of $H_2\mathbf{9}^{2+}$ were measured by taking advantage of the spectroscopic differences seen for the various protonated forms of sapphyrin. By adjusting the pH of an aqueous solution of **9** through a wide range (2.5 to 13.5) and plotting the absorbances at all the maxima listed in Table 4 against pH, the pK_a's of $H_2\mathbf{9}^{2+}$ were determined to be 5.8 ± 0.2 and 11.3 ± 0.3. These are notably higher than the pK_a values of 4.8 and 8.8 reported for a water soluble, meso-free, β-alkyl substituted sapphyrin studied under similar conditions,[13] a difference we attribute to the presence of electron-donating meso-aryl substituents in **9**.

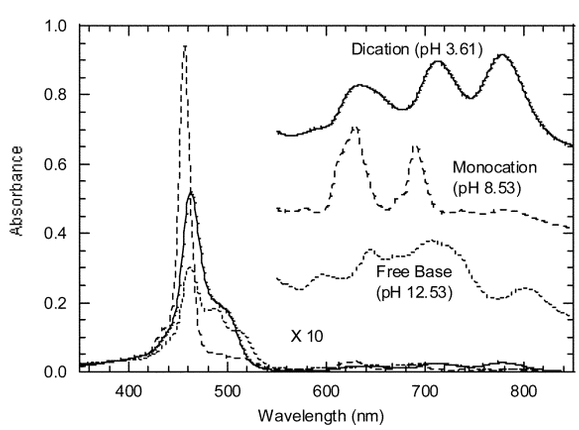

Fig. 9 Visible absorbance spectra of buffered aqueous solutions of sapphyrin **9** recorded at various pH values. The observed spectra are ascribed to the dicationic ($H_2\mathbf{9}^{2+}$), the monocationic ($H\mathbf{9}^{+}$), and the free base (**9**) forms. The absorbances in the Q-band region (550–850 nm) are enhanced 10-fold and offset for clarity. Phosphate buffer adjusted with sodium hydroxide was used to generate the pH 3.61, 8.53, and 12.53 solutions; see experimental section for details.

Table 4 Visible absorbance and emission maxima for the three protonation states of **9** observed in buffered aqueous solutions at various pH. Excitation wavelengths corresponding to the Soret λ_{max} were used to obtain the emission data

Protonation state (pH)	Absorbance maxima/nm	Emission maxima/nm (relative intensities)
$H_2\mathbf{9}^{2+}$ (3.61)	463, 630, 715, 775	700 (0.40)
$H\mathbf{9}^{+}$ (8.53)	456, 630, 690	695 (1.0), 768 (0.20)
9 (12.53)	461, 485, 515 595, 645, 710, 805	694 (0.18), 758 (0.14)

Ring inversion behavior of meso-diaryl sapphyrin

While "ruffling" and other deviations from planarity have been observed for highly substituted porphyrins and certain porphyrin–metal complexes, porphyrin is known to be a relatively rigid system, and conformations in which a pyrrole subunit is rotated such that the nitrogen is oriented towards the exterior of the macrocycle have not been observed in normal porphyrins (*i.e.*, ones containing pyrroles linked through 2 and 5 positions).[1–3] The same is true for most β-alkyl substituted porphyrins.[35] By contrast, meso-aryl sapphyrins are known to adopt conformations in which one pyrrole is inverted (*e.g.*, exists in a form where the NH atoms point away from the macrocyclic center).[31,32] This inverted conformation has been observed in solutions of the free base form of tetraaryl sapphyrins as well as, under certain conditions, in solutions of the protonated form. In both cases, inversion is characterized by large changes in the ^{1}H-NMR spectrum, particularly for the signals corresponding to the NH and β-Hs of the inverted pyrrole.[31–36] Similar conclusions regarding pyrrole ring inversion were reported by Dolphin for the free base form of 10,15-diphenyl sapphyrin, a system that differs from **7** only in that it lacks alkyl substituents on the bipyrrole subunit (positions 2, 3, 22, and 23).[22] Given this precedent, it was not surprising that evidence consistent with inversion was observed in the case of the free base forms of diaryl sapphyrins **8** and **9**; specifically the resonance in the ^{1}H-NMR spectra corresponding to the β-H's on the central pyrrole of the tripyrrane subunits of the two sapphyrins was found to shift from 9.3 ppm to −0.6 ppm in CD_2Cl_2 after washing with a solution of NaOD in D_2O. This finding is consistent with the assumption that the observed flipping reflects the presence of the meso-aryl subsitituents and is not dependent on whether or not the pyrroles in the bipyrrole subunit bear small alkyl substituents.

Conclusions

The aggregation behavior of several meso-free, β-alkyl substituted and meso-disubstituted water soluble sapphyrin derivatives (**1**–**6** and **9**) in aqueous media was examined. Both classes of compounds were found to form H-type dimers and higher order aggregates in neutral aqueous solution. However, in contrast to what was observed for the β-alkyl substituted sapphyrins, sapphyrin **9** and its organic soluble analogues, **7** and **8**, were found to form J-type dimers in methanol. Although the type of dimer formed in methanol differs between the meso-free, deca-β-substituted sapphyrins (H-type) and the meso-diaryl substituted sapphyrins (J-type), the strength of the interactions leading to dimer formation is on the same order of magnitude.

In aqueous media, the extent of aggregation was found to be anion dependent, a critical finding that underscores the ability of protonated sapphyrins to act as anion binding agents. These anion dependent effects were particularly noteworthy in the case of phosphate anions. For instance, addition of sodium phosphate to pH 7.0 solutions of sapphyrins **1**–**6** was found to give rise to an increase in the concentration of the monomeric form. Presumably, this reflects the fact that binding of phosphate to the protonated sapphyrin core helps stabilize the monomer in solution, allowing some of the sapphyrin originally involved in π-stacking to be liberated in the form of an anion-bound monomer. Since the monomeric forms of sapphyrin are highly fluorescent relative to the dimer and higher order aggregates, the addition of phosphate anions to solutions of these sapphyrins induces a large increase in the fluorescence emission. This increase in emission correlates well with the increase in phosphate concentration. Effective association constants could thus be calculated using standard 1 : 1 curve fitting methods and were found to range from *ca.* 6 to 19 M^{-1}. While these values are low, the dramatic changes in emission intensity associated with phosphate binding allow small changes in concentration to be detected, even at a dynamic range that is far lower than would be expected on the basis of binding constants alone. For instance, over the physiologically important concentration regime of 0–7 mM, the emission intensity of sapphyrin **1** was seen to increase by a factor of 3.

The concentration of chloride anion present in the aqueous sapphyrin solutions was also found to affect the aggregation equilibrium. Upon addition of this anion, changes in the visible absorbance profiles are observed that are consistent with increases in the concentration of the dimeric form. However, no spectroscopic evidence consistent with the build-up of an appreciable concentration of the monomeric form was obtained even at very high chloride anion concentrations (*e.g.*, 1 M). Thus, while the addition of chloride affects the aggregation equilibrium, it does not interfere with the ability of these sapphyrins to respond quantitatively to changes in phosphate anion concentration. Indeed, the effective association constants for phosphate binding by sapphyrins **1** and **6** at pH 7 (25 mM PIPES buffer) were found to be essentially unchanged in the presence and absence of 150 mM NaCl. Based on these observations, we propose that water soluble sapphyrins could have a role to play as phosphate anion sensors in various biological milieus, including in solid tumors where they are known to localize.[20] They could thus serve to complement other optical-based approaches to phosphate and phosphate-type anion sensing.[37–44]

Experimental

Tetrahydrofuran (THF) was dried by distillation under nitrogen over sodium. Spectroscopic grade CH_2Cl_2 and CH_3OH used for UV-vis and fluorescence spectroscopic experiments was obtained from EM Science. Aqueous solutions for these experiments were prepared using water that was purified using a three stage filtration system made by US Filter, Inc. All other reagents were purchased from Aldrich, Sigma, or TCI, Inc. and used as received. TLC analyses were performed on precoated silica gel or aluminum oxide plates obtained from Whatman International, Inc. Flash chromatography was performed using Merck silica gel 60, Scientific Adsorbents, Inc. flash silica gel, or Aldrich Brockmann 1 activated neutral aluminum oxide as the solid support. Proton and ^{13}C-NMR spectra were measured at 25 °C on a GE QE-300 spectrometer at 300 (proton) and 75 MHz (carbon), a Varian Inova 500 spectrometer at 500 MHz (proton) and 125 MHz (carbon) or a Bruker AMX-500 spectrometer at 500 MHz (proton) and 125 MHz (carbon). Chemical shifts are reported in parts per million using the solvent as standard. UV-vis spectra were recorded on a Beckman DU-650 spectrophotometer. Fluorescence spectra were measured at 25 °C using an Instruments SA, Inc. Fluorolog FL3-11 spectrophotometer. Low resolution FAB+ and CI+ mass spectra were obtained on a Finningan MAT TSQ 70

mass spectrometer. High resolution FAB+ and CI+ mass spectra were obtained on a VG ZAB2-E mass spectrometer. Elemental analyses were performed either by Atlantic Microlabs or by the Analytical Chemistry Department at the Institute for Chemical Technology in Prague.

Preparation of sapphyrins

The polyamine sapphyrins **2**–**4**[20,21] and the diphenyl sapphyrin **7**[22,23] were prepared by literature procedures.

8,17-Bis(2-(1-amino-1-deoxy-D-sorbitol)carbonylethyl)-3,12,13,22-tetraethyl-2,7,18,23-tetramethylsapphyrin (5)

Sapphyrin diacid **10** (55 mg, 72 μmol) and 1-(3-dimethylaminopropyl)-3-ethylcarbodiimide hydrochloride (EDC; 69 mg, 360 μmol) were dissolved in 20 mL DMF in a round bottom flask. 1-Hydroxybenzotriazole (HOBT; 47 mg, 360 μmol) was added, and the reaction was protected from light with aluminum foil and stirred for 30 min. A solution of 1-amino-1-deoxy-D-sorbitol (**11**; 130 mg, 720 μmol), was prepared in a 2 : 1 mixture of DMF and water, and added to the reaction dropwise. The reaction was stirred for 48 h at room temperature, and then the solvents were removed by vigorous stirring under high vacuum with gentle heating (40 °C). The residue was redissolved in dilute HCl (0.05 M) and loaded onto a Supelco Supelclean LC-18 cartridge, which was flushed with deionized water to remove the urea salts and residual aminosorbitol. The cartridge was then eluted with CH_3OH, and the green solution containing the crude sapphyrin product was collected and stripped of solvent. This product was then redissolved in a 5 : 1 CH_2Cl_2 : CH_3OH mixture and loaded onto a very short (*ca.* 2.5 cm) column of silica gel. This column was washed with a 5 : 1 CH_2Cl_2 : CH_3OH mixture to remove residual starting material, and then with CH_3OH. The volume of the green CH_3OH solution was reduced to approximately 5 mL before being layered with diethyl ether and allowed to sit for several days. The product sapphyrin **5** (10 mg, 13%) was collected as a dark green solid (Found: C, 59.41; H, 7.29; N, 8.82. $C_{54}H_{75}N_7O_{12}$·2HCl requires: C, 59.66; H, 7.14; N, 9.02.); ^{1}H-NMR (500 MHz; 25% CD_3OD in $CDCl_3$) δ 2.14 (6H, t, CH_2CH_3), 2.27 (6H, t, CH_2CH_3), 3.13 (4H, t, CH_2CON), 3.23 (6H, s, CH_3), 3.34 (6H, s, CH_3), *ca.* 3.38 (8H, m, $CHOH$), 4.11 (4H, dd, CH_2OH), 4.31 (4H, dd, CH_2OH), 4.57 (4H, q, CH_2CH_3), 4.79 (4H, q, CH_2CH_3), 5.09 (4H, t, CH_2CH_2CON), 10.45 (2H, s, meso-H), 11.72 (2H, s, meso-H); ^{13}C-NMR (125 MHz; CD_3OD) δ 12.74, 15.43, 17.41, 18.28, 20.68, 22.61, 23.23, 34.41, 35.86, 38.82, 61.28, 65.69, 70.26, 71.49, 72.69, 89.44, 91.09, 98.54, 125.84, 127.39, 129.75, 132.23, 132.60, 134.76, 137.67, 141.85, 143.72, 156.64; HRMS m/z (FAB+) 1014.557099 (M^+ + H. $C_{54}H_{76}N_7O_{12}$ requires 1014.555197).

8,17-Bis(2-(N-methyl-1-amino-1-deoxy-D-sorbitol)carbonylethyl)-3,12,13,22-tetraethyl-2,7,18,23-tetramethylsapphyrin (6)

The procedure described for **5** was also used for the synthesis and purification of **6**. The same amounts of materials were used, except that N-methyl-1-amino-1-deoxy-D-sorbitol (**12**, 140 mg, 720 μmol) was used instead of 1-amino-1-deoxy-D-sorbitol (**11**). Sapphyrin **6** (8 mg, 10%) was collected as a dark green solid (Found: C, 60.07; H, 7.45; N, 8.61. $C_{56}H_{79}N_5O_{12}$·2HCl requires C, 60.31; H, 7.32; N, 8.79); ^{1}H-NMR (500 MHz; CD_3OD) δ 2.01 (6H, t, CH_2CH_3), 2.14 (6H, t, CH_2CH_3), 3.15 (4H, t, CH_2CON), 3.17 (6H, s, NCH_3) 3.64 (6H, s, CH_3), 3.66 (6H, s, CH_3), ca. 3.68 (8H, m, $CHOH$), 3.77 (4H, dd, CH_2OH), 3.82 (4H, dd, CH_2OH), 4.03 (4H, q, CH_2CH_3), 4.13 (4H, q, CH_2CH_3), 4.39 (4H, t, CH_2CH_2CON), 10.55 (2H, s, meso-H), 10.81 (2H, s, meso-H); ^{13}C-NMR (125 MHz; CD_3OD) δ 13.31, 16.21, 19.91, 19.24, 21.84, 22.03, 23.95, 24.47, 33.91, 34.37, 36.50, 37.31, 37.57, 52.71, 53.20, 64.65, 69.61, 72.10, 72.24, 72.92, 128.40, 128.85, 131.67, 133.83, 139.01, 142.29, 144.06, 174.98; HRMS m/z (FAB+) 1042.587785 (M^+ + H. $C_{56}H_{80}N_7O_{12}$ requires 1042.586497).

10,15-Bis(3,5-di-*tert*-butylphenyl)-3,22-diethyl-2,23-dimethylsapphyrin (8)

Pyrrole (153 μL, 2.20 mmol), 3,5-di-*tert*-butylbenzaldehyde (320 mg, 1.47 mmol), and bisformyl bipyrrole **15** (200 mg, 0.73 mmol) were added to a round bottom flask containing 250 mL CH_2Cl_2 and a magnetic stirrer. Following the addition of *p*-toluenesulfonic acid (50 mg), the reaction vessel was protected from light by covering it with aluminum foil and stirred overnight. The next morning, DDQ (2,3-dichloro-5,6-dicyano-1,4-benzoquinone; 56 mg, 0.73 mmol) was added and the reaction was stirred for 20 min. The bulk of the polymeric by-products were removed by passing the raw material through a neutral alumina column using 0–1% CH_3OH in CH_2Cl_2 as the eluent. The crude product obtained in this way was subject to two additional rounds of chromatographic purification using silica gel as the solid support and 1–5% CH_3OH in CH_2Cl_2 as the eluent. This product was further purified by recrystallization from CH_2Cl_2/hexane to give **8**·2HCl (33 mg, 5%) as lusterous blue crystals (Found C, 76.63; H, 7.87; N, 7.70. $C_{58}H_{69}H_5$·2HCl requires C, 76.29; H, 7.98; N, 7.51); λ_{max}(CH_2Cl_2) 463 (log ε 5.68), 631 (4.13), 708 (4.28); ^{1}H-NMR (300 MHz; CD_2Cl_2) δ −4.14 (s, 4H, NH), −3.40 (s, 1H, NH), 1.70 (s, 36H, *t*-Bu), 2.24 (t, 6H, CH_2CH_3), 4.25 (s, 6H, CH_3), 4.64 (q, 4H, CH_2CH_3), 8.14 (s, 2H, phenyl H), 8.64 (s, 4H, phenyl H), 9.28 (s, 2H, β-H), 9.62 (d, 2H, β-H), 10.25 (d, 2H, β-H), 11.81 (s, 2H, meso-H); ^{13}C-NMR (75 MHz; CD_2Cl_2) δ 16.0, 17.8, 21.1, 31.9, 35.5, 101.9, 116.3, 122.5, 128.8, 130.2, 130.4, 130.6, 131.4, 132.4, 132.5, 135.2, 140.0, 140.4, 143.3, 145.4, 149.4; HRMS m/z (FAB+) 836.561312 (M^+ + H. $C_{58}H_{70}O_5$ requires 836.563123).

10,15-bis[3,5-bis[2-[2-(2-Methoxyethoxy)ethoxy]ethoxy]-phenyl]-3,22-diethyl-2,23-dimethyl sapphyrin (9)

Diaryl tripyrrane **14** (102 mg, 0.10 mmol) and bisformyl bipyrrole **15** (27 mg, 0.10 mmol) were dissolved in 250 mL CH_2Cl_2. The reaction flask was protected from light with aluminum foil, and *p*-toluenesulfonic acid (10 mg) was added. After stirring overnight, DDQ (23 mg, 0.10 mmol) was added to the reaction mixture. Following 20 min of stirring, the reaction was washed with NaOH (0.5 M) and HCl (1 M), dried over Na_2SO_4, and stripped of solvents. The bulk of the polymeric by-products were removed by passing the raw material through a neutral alumina column using 0–1% CH_3OH in CH_2Cl_2 as the eluent. The crude product obtained in this way was subject to two additional rounds of chromatographic purification using silica gel as the solid support and 1–5% CH_3OH in CH_2Cl_2 as the eluent. After collecting the appropriate fraction and removal of solvent, **9**·2HCl was isolated in the form of a thick, lustrous blue oil (8 mg, 9%). This sapphyrin was also prepared *via* the 'one pot' method. In this case, pyrrole (153 μL, 2.20 mmol), 3,5-bis[2-[2-(2-methoxyethoxy)ethoxy]ethoxy]-benzaldehyde (630 mg, 1.47 mmol), and bisformyl bipyrrole **15** (200 mg, 0.73 mmol) were added to a round bottom flask containing 250 mL CH_2Cl_2 and a magnetic stirrer. After adding *p*-toluenesulfonic acid (50 mg) and protecting the reaction vessel from light by covering it with aluminum foil, the reaction mixture was stirred overnight. The next morning, DDQ (2,3-dichloro-5,6-dicyano-1,4-benzoquinone; 56 mg, 0.73 mmol) was added and the reaction was stirred for 20 min. The same workup and chromatographic purification described above was then employed to isolate **9**·2HCl (59 mg, 6%) as a lusterous blue oil (Found C, 63.44; H, 7.35; N, 4.88. $C_{70}H_{93}N_5O_{16}$·2HCl requires C, 63.05; H, 7.18; N, 5.32); λ_{max}(CH_2Cl_2)/nm 464 (log ε 5.66), 631 (4.06), 704 (4.20); ^{1}H-NMR (300 MHz; $CDCl_3$) δ −4.48 (s, 2H, NH), −4.35 (s, 2H, NH), −3.98 (s, 1H, NH), 2.37 (t, 6H, CH_2CH_3), 3.48 (s, 12H, OCH_3), 3.61 (t, 8H, CH_2), 3.69 (t, 8H, CH_2), 3.72 (t, 8H, CH_2), 3.80 (t, 8H, CH_2), 4.11 (t,

8H, CH_2), 4.25 (s, 6H, CH_3), 4.44 (t, 8H, CH_2), 4.58 (q, 4H, CH_2CH_3), 7.20 (m, 2H, phenyl H), 7.96 (s, 4H, phenyl H), 9.54 (s, 2H, β-H), 9.70 (d, 2H, β-H), 10.28 (d, 2H, β-H), 11.85 (s, 2H, meso-H); ^{13}C-NMR (75 MHz, $CDCl_3$) δ 15.8, 17.5, 21.1, 59.0, 68.6, 70.2, 70.8, 71.2, 72.1, 102.4, 102.9, 114.5, 116.9, 130.0, 130.7, 131.0, 131.3, 131.9, 135.5, 139.7, 144.0, 147.0, 158.7; HRMS *m/z* (FAB+) 1260.669483 (M^+ + H. $C_{70}H_{94}N_5O_{16}$ requires 1260.669558).

5,10,15,20-tetra[3,5-bis[2-[2-(2-Methoxyethoxy)ethoxy]ethoxy] phenyl] porphyrin (16)

From the reaction sequence that produced the 10,15-diaryl substituted sapphyrin **9**, porphyrin **16** was isolated as a lusterous purple oil (Found C, 61.41; H, 7.35; N, 2.86. $C_{100}H_{142}N_4O_{32}$ requires C, 62.81; H, 7.48; N, 2.93); ^{1}H-NMR (300 MHz; $CDCl_3$) δ −2.83 (s, 2H, NH), 3.35 (s, 24H, OCH_3), 3.52 (t, 16H, CH_2), 3.66 (t, 16H, CH_2), 3.73 (t, 16H, CH_2), 3.81 (t, 16H, CH_2), 3.98 (t, 16H, CH_2), 4.35 (t, 16H, CH_2), 6.99 (t, 4H, phenyl H), 7.45 (d, 8H, phenyl H), 8.95 (s, 8H, β-H); ^{13}C-NMR (75 MHz, $CDCl_3$) δ 59.3, 68.3, 70.2, 70.9, 17.1, 71.3, 72.3, 102.0, 115.2, 120.1, 131.3, 131.5, 144.3, 158.5; HRMS *m/z* (FAB+) 1911.968057 (M^+ + H. $C_{100}H_{143}N_4O_{32}$ requires 1911.968545).

Binding studies

The effective equilibrium constants for sapphyrins **1**–**6** with phosphate (*cf*. Table 1) were determined from fluorescence emission titration studies carried out in aqueous solutions containing 25 mM PIPES buffer (pH 7.0) and 150 mM NaCl. The emission intensity at 690 nm was observed while using an excitation wavelength of 450 nm. Data fits were performed using the computer software package KaleidaGraph 3.52 assuming a 1:1 binding model. Specifically, equation 12.5 of ref. 26 was computer fit using F/F_0 and $[P_i]$ as the dependent and independent variables, respectively. The curve fits used to generate the effective equilibrium constants given in Table 1 are provided in the supporting material.[14,26] In these titrations, the sapphyrin concentration was held constant at 3 μM while the concentration of phosphate anion was increased from 0 to 100 mM. Within this concentration regime ($[P_i]$>>[Sap]), the simplifying assumption that $[P_i] \approx [P_i]_0$ holds. The phosphate anion was added in the form of aqueous solutions generated from NaH_2PO_4 by dissolving in 25 mM PIPES buffer containing 150 mM NaCl and then bringing to a pH of 7.0 by the addition of NaOH.

Dimerization studies

The dimerization constants of sapphyrins **7**–**9** in methanol, reported in Table 2, were determined using the method of Pasternack,[29] a protocol we have used previously to determine a dimerization constant of 1.4×10^4 M^{-1} for sapphyrin **17**.[12] Specifically, eqn. (8) of ref. 29 was computer fit with Kaleidagraph 3.52 using $A_0 - A$ and [Sap] as the dependent and independent variables, respectively. The curve fits used to generate the dimerization constants given in Table 2 are provided in the supporting material.

Crystal structure determination of sapphyrin 8

Single crystals of **8**·2HBr were grown from a CH_2Cl_2 solution layered with hexanes. $C_{66}H_{91}Br_2N_5O_2$, M = 1146.26, triclinic, a = 13.5011(4), b = 15.4181(4), c = 16.1110(5) Å, α = 102.337(2), β = 98.236(1), γ = 95.617(1)°, V = 3213.69(16) Å^3, T = 152(2) K, space group P-1, Z = 2, μ(Mo Kα) = 1.306 mm^{-1}, 18405 reflections measured, 11303 unique (R_{int} = 0.0486) which were used in all calculations. The final R indices were $R1$ = 0.113, $wR2$ = 0.158 (all data).

CCDC reference number 213468.

See http://www.rsc.org/suppdata/ob/b3/b306964h/ for crystallographic data in CIF or other electronic format.

pK_a determination

An aqueous solution of sapphyrin **9** (2 μM) containing 15 mM phosphoric acid, 100 mM NaCl (to maintain constant ionic strength), and 10 mM SDS surfactant (to inhibit formation of aggregates of **9**) was prepared. The pH of this solution was adjusted across a wide range (2.3–13) and absorbance spectra were collected every 0.2 pH units. The visible absorbance maxima (Soret and Q-bands) of each of the three protonation states (dication, $H_2\mathbf{9}^{2+}$; monocation, $H\mathbf{9}^+$, and free base, **9**) were plotted as a function of pH, and the inflection points of these graphs were taken to correspond to the pK_a's. This procedure was also repeated using a range of organic buffers (specifically, acetate, PIPES, TAPS, and CAPS; 5 mM each) in place of the phosphate buffer so as to cover a more-complete pH range. As a control, two different buffer systems were looked at in detail to determine if the presence of phosphate anions would affect the results. The first system was a simple phosphate buffer (15 mM, pK_a = 2.2, 7.1, 12.4), and the second system was a mixture (5 mM each) of acetate (pK_a = 4.8), PIPES (1,4-piperazinebis-(ethanesulfonic acid), pK_a = 6.8), TAPS (3-[[tris(hydroxymethyl)methyl]amino]-1-propanesulfonic acid, pK_a = 8.4), and CAPS (3-cyclohexylamino-1-propanesulfonic acid, pK_a = 10.4). No appreciable change in sapphyrin protonation behavior was seen when using these two buffers. pH values were measured using an Orion 720 digital pH meter, calibrated with pH 4.00 and 7.00 standard solutions.

Acknowledgements

This work was supported by the National Institute of Health (grant GM 58907 to J.L.S.) and Czech Republic grant MSM 223400008.

References

1 D. Dolphin, in *The Porphyrins*, Academic Press, New York, 1978, vol. 1–8.
2 K. M. Smith, in *Porphyrins and Metalloporphyrins*, Elsevier, Amsterdam, 1976.
3 K. M. Kadish, K. M. Smith, and R. Guilard, in *The Porphyrin Handbook*, Academic Press, San Diego, 2000.
4 A. Jasat and D. Dolphin, *Chem. Rev.*, 1997, **97**, 2267–2340.
5 J. L. Sessler and S. J. Weghorn, in *Expanded, Contracted and Isomeric Porphyrins*, Elsevier, Oxford, 1997.
6 C. A. Hunter and J. K. M. Sanders, *J. Am. Chem. Soc.*, 1990, **112**, 5525–5534.
7 D. L. Akins, H.-R. Zhu and C. Guo, *J. Phys. Chem.*, 1996, **100**, 5420–5425.
8 N. C. Maiti, S. Mazumdar and N. Periasamy, *J. Phys. Chem. B*, 1998, **102**, 1528–1538.
9 K. Kano, K. Fukuda, H. Wakami, R. Nishiyabu and R. F. Pasternack, *J. Am. Chem. Soc.*, 2000, **122**, 7494–7502.
10 R.-H. Jin, S. Aoki and K. Shima, *J. Chem. Soc., Faraday Trans.*, 1997, **93(22)**, 3945–3953.
11 K. Lang, P. Anzenbacher, P. Kapusta, V. Král, P. Kubát and D. M. Wagnerová, *J. Photochem. Photobiol., B*, 2000, **57**, 51–59.
12 B. G. Maiya, M. Cyr, A. Harriman and J. L. Sessler, *J. Phys. Chem.*, 1990, **94**, 3597–3601.
13 V. Král, H. Furuta, K. Shreder, V. Lynch and J. L. Sessler, *J. Am. Chem. Soc.*, 1996, **118**, 1595–1607.
14 B. L. Iverson, K. Shreder, V. Král, P. Sansom, V. Lynch and J. L. Sessler, *J. Am. Chem. Soc.*, 1996, **118**, 1608–1616.
15 V. J. Bauer, D. L. J. Clive, D. Dolphin, J. B. Paine III, F. L. Harris, M. M. King, J. Loder, S. W. C. Wang and R. B. Woodward, *J. Am. Chem. Soc.*, 1983, **105**, 6429–6436.
16 J. L. Sessler and J. M. Davis, *Acc. Chem. Res.*, 2001, **34(12)**, 989–997.
17 J. L. Sessler, M. Cyr, H. Furuta, V. Král, T. Mody, T. Morishima, M. Shionoya and S. Weghorn, *Pure Appl. Chem.*, 1993, **65**, 393–398.
18 V. Král and J. L. Sessler, *Tetrahedron*, 1995, **51**, 539–554.
19 B. L. Iverson, R. E. Thomas, V. Král and J. L. Sessler, *J. Am. Chem. Soc.*, 1994, **116**, 2663–2664.
20 V. Král, J. Davis, A. Andrievsky, J. Kralová, A. Synytsya, P. Poucková and J. L. Sessler, *J. Med. Chem.*, 2002, **45(5)**, 1073–1078.

21 J. L. Sessler, A. Andrievsky, P. I. Sansom, V. Král and B. L. Iverson, *Bioorg. Med. Chem. Lett.*, 1997, **7 (11)**, 1433–1436.
22 C. Brückner, E. D. Sternberg, R. W. Boyle and D. Dolphin, *Chem. Commun.*, 1997, 1689–1690.
23 J. L. Sessler, J. Lisowski, K. A. Boudreaux, V. Lynch, J. Barry and T. J. Kodadek, *J. Org. Chem.*, 1995, **60**, 5975–5978.
24 J. W. Bohn, *Annu. Rev. Phys. Chem.*, 1993, **44**, 37–60.
25 S. S. Zumdahl, in *Chemistry*, D. C. Heath and Company, Lexinton, MA, 2nd edn., 1995, p. A25.
26 K. A. Connors, in *Binding Constants. The Measurement of Molecular Complex Stability*, Wiley, New York, 1987, pp. 339–343.
27 M. Shionoya, H. Furuta, V. Lynch, A. Harriman and J. L. Sessler, *J. Am. Chem. Soc.*, 1992, **114**, 5714–5722.
28 D. Voet and J. G. Voet, in *Biochemistry*, John Wiley & Sons, Inc., New York, 2nd edn., 1995.
29 R. F. Pasternack, *Ann. N. Y. Acad. Sci.*, 1973, **206**, 614–630.
30 R. C. Weast and M. J. Astle, in *CRC Handbook of Chemistry and Physics*, CRC Press, Inc., Boca Raton, FL, 63rd edn., 1982, p. F-179.
31 P. J. Chmielewski, L. Latos-Grażyński and K. Rachlewicz, *Chem. Eur. J.*, 1995, **1**, 68–73.
32 K. Rachlewicz, N. Sprutta, L. Latos-Grażyński, P. J. Chmielewski and L. Szterenberg, *J. Chem. Soc., Perkin Trans. 2*, 1998, 959–967.
33 A. Srinivasan, S. K. Pushpan, M. R. Kumar, S. Mahajan, T. K. Chandrashekar, R. Roy and P. Ramamurthy, *J. Chem. Soc., Perkin Trans. 2*, 1999, 961–968.
34 L. Szterenberg and L. Latos-Grażyński, *J. Phys. Chem. A*, 1999, **103**, 3302–3309.
35 K. Rachlewicz, L. Latos-Grażyński, A. Gebauer, A. Vivian and J. L. Sessler, *J. Chem. Soc., Perkin Trans. 2*, 1998, 2189–2195.
36 N. Sprutta and L. Latos-Grażyński, *Org. Lett.*, 2001, **3(12)**, 1933–1936.
37 M. E. Huston, E. U. Akkaya and A. W. Czarnik, *J. Am. Chem. Soc.*, 1989, **111**, 8735–8737.
38 A. W. Czarnik, *Acc. Chem. Res.*, 1994, **27**, 302–308.
39 S. Watanabe, O. Snogawa, Y. Komatsu and K. Yoshida, *J. Am. Chem. Soc.*, 1998, **120**, 229–230.
40 S. Nishizawa, Y. Kato and N. Teramae, *J. Am. Chem. Soc.*, 1999, **121**, 9463–9464.
41 S. L. Wiskur, H. Ait-Hssou, J. J. Levine and E. Anslyn, *Acc. Chem. Res.*, 2001, **34**, 963–972.
42 M. S. Han and D. H. Kim, *Angew. Chem. Int. Ed.*, 2002, **41(20)**, 3809–3811.
43 S. Shao, Y. Gou, L. He, S. Jiang and X. Yu, *Tetrahedron Lett.*, 2003, **44**, 2175–2178.
44 L.-J. Kuo, J.-H. Liao, C.-T. Chen, C.-H. Huang, C.-S. Chen and J.-M. Fang, *Org. Lett.*, 2003, **5(11)**, 1821–1824.